High Resolution Transmission Electron Microscopy of Some Catalysts

G. W. Qiao, J. Zhou, and K. H. Kuo

Institute of Metal Research, Academia Sinica, Wenhua Road, Shenyang, P.R. China

Z. Naturforsch. **41 a**, 478–482 (1986); received November 30, 1985

Application of high resolution electron microscopy (HREM) to the study of Pt-Sn/γ-Al_2O_3 supported catalyst, zeolites, iron catalyst for ammonia synthesis, rare-earth oxide catalysts, etc., is described. Micro-twins, dislocations and other crystallographic imperfections are observed. Moreover, the structure images of channels representing columns of cages in several kinds of zeolites as well as radiation damage processes in them have been recorded in situ. The observed images of zeolites were found to be in good agreement with the structure model projections and computer simulated images.

Key words: HRTEM of catalysts.

1. Introduction

The great merit of HREM is that it can elucidate structure information in real space and at the atomic level. HREM is also especially useful in evaluating structural transformations and clarifying the nature of crystalline imperfections [1].

In principle the HREM technique is particularly suitable for probing the microstructure of catalysts but its application, until recently, has been limited by two experimental difficulties. One is the high sensitivity of some catalysts (especially zeolites) to the electron beam irradiation. The other is that some extremely fine particles (supported catalysts) are rather difficult to image directly because their sizes are too small to make the necessary orientation adjustment, which is based on the symmetry of the electron diffraction pattern. Such an adjustment is quite difficult if not impossible. Moreover, the scattering in the support may also destroy the phase contrast of the specimen under examination. However, techniques have now been developed which, in favourable circumstances, have made possible the direct lattice imaging of the catalysts at sub-nanometer or even atomic level [2–7].

The present paper describes the preliminary results of HERM observations made on Pt-Sn bimetallic catalyst, zeolites, iron catalyst for ammonia synthesis and rare-earth oxide catalysts in our HREM laboratories during last two years.

Reprint requests to Dr. G. W. Qiao, presently Fritz-Haber-Institut der Max-Planck-Gesellschaft, Faradayweg 4–6, D-1000 Berlin 33.

2. Experimental Methods

Specimens of industrial catalysts (Pt-Sn bimetallic fine particles [8, 9], zeolites [10, 11], rare-earth oxides [12], iron catalysts [13], etc.) for HREM examination were made by the following methods: (1) The industrial catalysts were ground in an agate mortar and dispersed in methanol. Thin fragments were then collected on a carbon film (specially made, extremely thin) supported on a copper grid. (2) The supported small particles (Pt-Sn/γ-Al_2O_3) were treated with HF acid, the γ-alumina support was dissolved and the remained metal particles were dispersed on freshly cleaved rock salt surfaces and then extracted with extremely thin, vacuum deposited carbon foils. (3) The catalysts were imbedded in methyl methacrylate and butyl methacrylate (1:1) at 45–60 °C for 24 hrs and the probes were then sliced into thin foils of a thickness of about 5–10 nm by chance in the edge parts, using an ultra-microtome. The foils were then supported directly on copper grids. Since untreated zeolite catalysts are very beam sensitive, the specimens were put into a vacuum evaporator at 10^{-5} Torr for several days before EM observation in order to remove moisture and to improve the stability under the electron beam irradiation [14].

0340-4811 / 86 / 0300-0478 $ 01.30/0. – Please order a reprint rather than making your own copy.

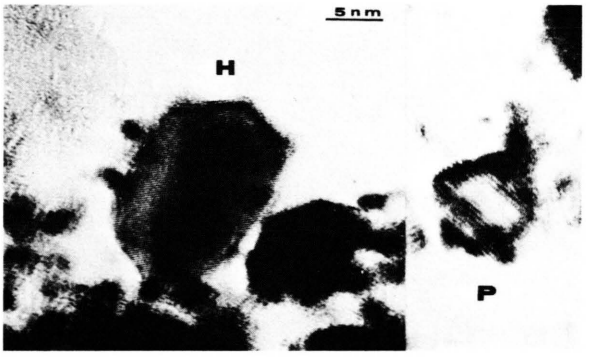

Fig. 1. Extracted hexagonal (H) and pentagonal (P) particles in a Pt-Sn bimetallic catalyst.

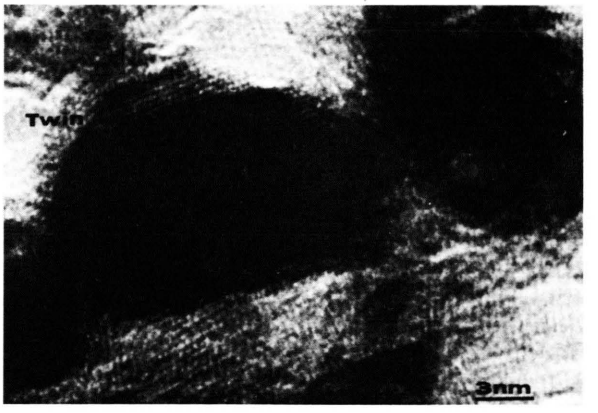

Fig. 3. Microtwins in an industrial Pt-Sn/γ-Al_2O_3 supported catalyst particle.

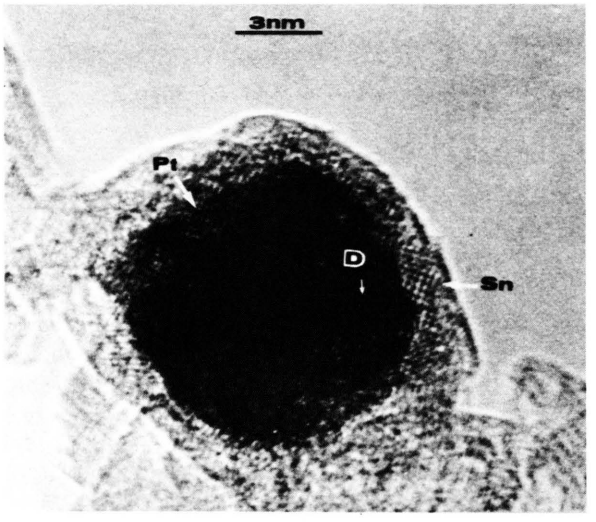

Fig. 2. An industrial Pt-Sn catalyst particle with a high Sn content. In addition to Pt crystal with [100] orientation at Pt, β-tin crystal with [001] orientation also occurs at Sn. In region D a dislocation is present.

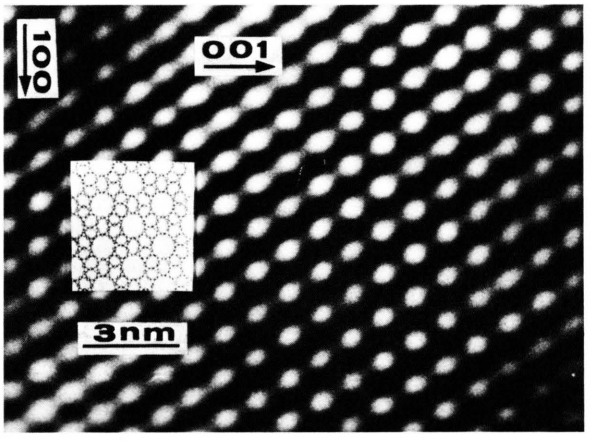

Fig. 4. Channel images of ZSM-5 zeolite in [010] direction, which is consistent with the projected structure model (inset).

It is advantageous to use an image intensifier for image recording at a rather weak illumination and a low dose of electron irradiation. Furthermore, continuous observation of phase transformation as well as radiation damage processes can be recorded directly.

The HREM observations were carried out at 200 kV using a JEM-200 CX electron microscope equipped with a high resolution top entry goniometer stage. Mainly, the structure images were recorded at a magnification of $5.3-8.5 \times 10^5$ times using an objective aperture corresponding to a radius of 0.55 $Å^{-1}$ in the diffraction pattern.

Computer simulated images of the zeolites were calculated by using the multi-slice method with a programme written by Ishizuka [15]. The parameters used were as follows: spherical aberration coefficient: 1.2 mm; focus spread due to chromatic aberration: 3 nm; incident beam convergence: 0.4 mrad; number of diffracted beams included in the dynamic diffraction calculation: 964; value of defocus: − 60 nm.

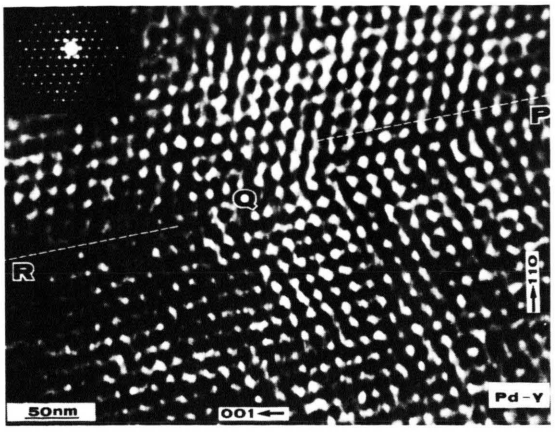

Fig. 6. Coherent twin boundaries (at P and R) and incoherent twin boundary (at Q) in Pd-Y zeolite. The inset is the corresponding SAED pattern.

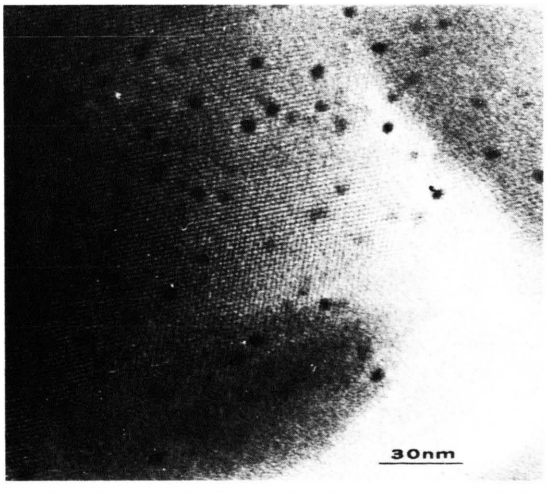

Fig. 7. Clusters (dark spots) of Pd atoms in Pd-Y zeolite. The white spots are the channel images.

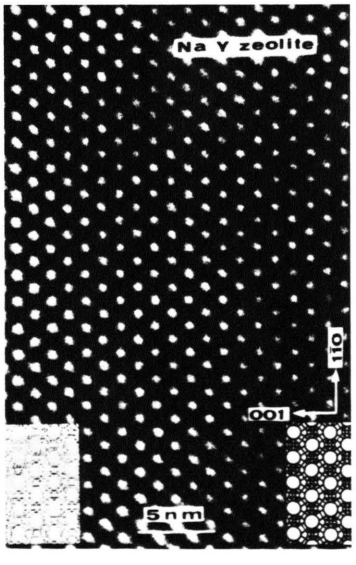

Fig. 5. Channel image of Na-Y zeolite in [110] direction. The lower right inset is the structure model projection. The lower left one is the computer simulated image.

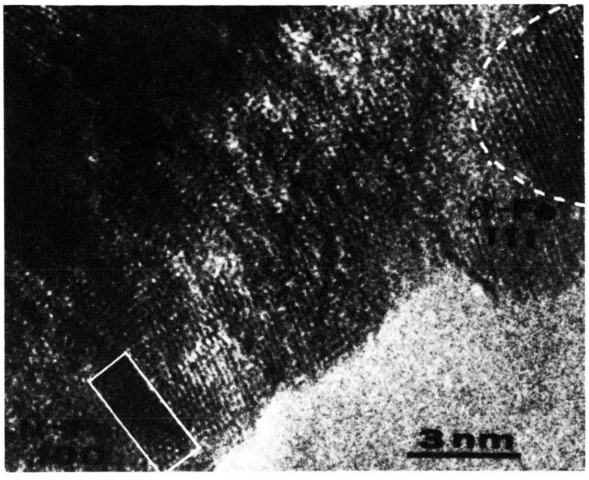

Fig. 8. The lattice images of α-iron particles in [100] and [111] orientations.

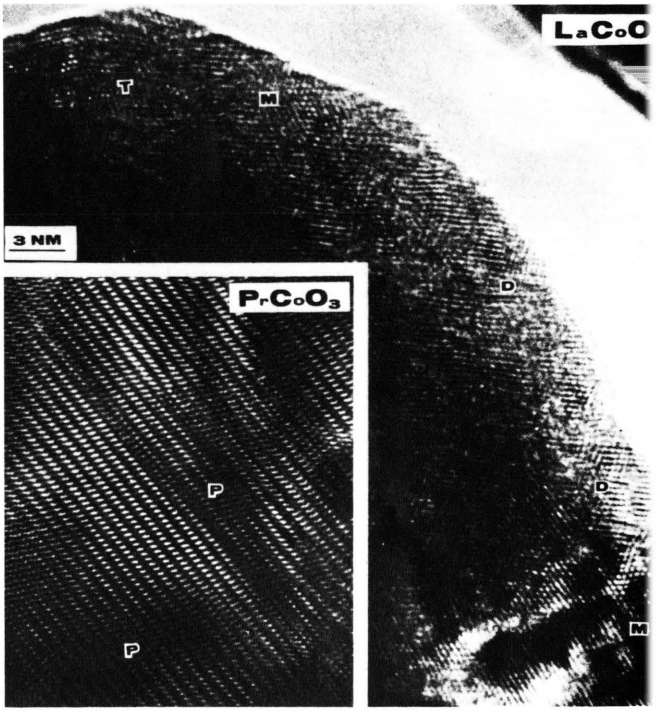

Fig. 10. The planar faults in $PrCoO_3$ catalyst.

Fig. 9. Microdomains (M), n twins (T) and dislocations ($LaCoO_3$ catalyst.

3. Results and Discussions

1. Pt-Sn/γ-Al_2O_3 Small Particles [16]

The supported metal catalyst used was in a highly dispersed state and was found consisting of very fine particles (1–20 nm in size). HREM observations have revealed that the fine Pt-Sn particles are microcrystallites. Some of them have regular shapes, such as hexagons and pentagons (Fig. 1), in which one- or two-dimensional lattice fringes can clearly be seen. SAED patterns showed that the fine particles with low Sn content are the solid solution of Sn in Pt matrix with a f.c.c. structure; when the Sn content is high, however, small particles of β-Sn with a b.c.t. structure have been observed. All of them were also confirmed by the high resolution lattice imaging. Figure 2 shows that the particle is polycrystalline with clear two-dimensional lattice fringes. This is consistent with the [100] atom projection of platinum in the region Pt (the nearest atom spacing is about 0.2 nm) while that in the region Sn agrees with the [001] atom projection of β-tin (the nearest atom spacing is about 0.3 nm). Meanwhile, a dislocation in region D can also be observed. Although the particle is as small as several nanometers in size, dislocations may still exist. In addition, microtwins do exist in such small particles in which, similar to well grown crystals, the {111} twinning plane and the mirror symmetry relationship of lattice planes can be seen (Figure 3). Moreover, some multiple twin particles have also been found.

2. Zeolites [16]

The channel structures of ZSM-5, Na-Y, USY, Pd-Y, HY and RE-Y zeolites have been examined by means of HREM. Figure 4 shows the channel structure image of an industrial ZSM-5 zeolite, which is in good agreement with the structure projection along the [010] direction shown as an inset. Channel structure images have also been observed in Na-Y zeolite (Figure 5). The lower right inset is the atomic projection along the [110] direction of the structure model, and the lower left one is the computer simulated image along the [110] projection with Scherzer defocus of −60 nm. All of them are in good agreement with each other. Twins were observed in Na-Y zeolite and some other cation exchanged Y zeolites. Figure 6 shows the twinning structure with an inset of the corresponding SAED pattern in Pd-Y zeolite. Both coherent and incoherent twin boundaries can be seen. This kind of incoherent twin boundary has also been observed in RE-Y and HY zeolites. It seems that incoherent twin boundaries are apt to occur when Na is substituted by other cations, such as Pd, rare-earth element, etc. Radiation damage in the zeolites is common and the processes have been recorded by a video system. At the beginning, only a few image spots disappeared, then they gradually grew as separated islands and finally merged, the whole field being amorphous. Moreover, if the exchanged cations are in excess, they may form separated clusters as seen in Pd-Y zeolite with excessive Pd atoms (Figure 7).

3. Iron Catalyst for Ammonia Synthesis [17]

The pellet shape A6 type iron catalyst promoted with $K_2O-CaO-Al_2O_3$ was observed in the as-reduced state by means of HREM. The pores are clearly visible with sizes of 5–100 nm. The hydrogen and nitrogen molecules have to diffuse in and ammonia out through the pores. SAED studies revealed that the interior of the catalyst consists of pure α-iron particle and there were no indications of alloying. HREM observations showed that the α-iron particles reduced from magnetite by hydrogen are about 2–30 nm in size; two-dimensional lattice images of α-Fe in [100] and [111] orientations have been observed (Figure 8). These small particles may provide the active sites for the chemisorption of nitrogen. Moreover, the surrounding matrix support of α-Fe_2O_3 was identified by the SAED patterns and also by high resolution direct imaging.

4. Rare-Earth Oxide Catalysts [18]

Rare-earth oxides $LaCoO_3$, $CeCoO_3$, $PrCoO_3$ and $SrCoO_3$ with catalytical ability were studied by HREM. X-ray and electron diffraction studies showed that they all have the perovskite structure. HREM observations indicated that there are a great number of crystalline imperfections in the rare-earth oxide catalysts. Figure 9 shows some micro-domains (M), micro-twins (T) and dislocations (D) observed in $LaCoO_3$. Figure 10 shows some planar faults in $PrCoO_3$. The planar faults

have also been frequently found in other kinds of RE-oxides. No obvious differences were found among the different kinds of rare-earth elements in their effects on the structure and imperfections. It seems that samples with higher activities have more imperfections.

4. Conclusions

The Pt-Sn bimetallic catalyst particles are crystalline in nature and micro-twins occur frequently. Sometimes, even dislocations can be found in such minute crystals. When the Sn content is high, Sn crystals occur together with Pt crystals in juxtaposition.

The tunnels and cages in zeolites can cearly be resolved by means of HREM. Twins have been identified and radiation damage has been followed during the observation.

Small particles of pure α-Fe have been found in the interior of the as-reduced promoted iron catalyst for ammonia synthesis.

Micro-domains, micro-twins and dislocations as well as some planar faults have been observed in the RE-oxide catalysts. No noticeable differences have been found among the different rare-earth elements in the influences on the structure faults.

Acknowledgements

The authors wish to thank the Dalian Institute of Chemical Physics and Changchung Institute of Applied Chemistry, Academia Sinica, and Liaohe Fertilizer Factory, for the generous supply of catalyst samples. Thanks are also due to Mr. B. C. Wang for his assistance in using ultra-microtome.

[1] J. M. Thomas, Proc. 8th Intern. Congr. Catal., West Berlin 1984, Vol. I, p. 33.
[2] A. Howie, L. D. Marks, and S. J. Pennycook, Ultramicroscopy **8,** 163 (1982).
[3] J. M. Cowley, J. C. Wheatley, and W. L. Kehl, J. Catal. **56,** 185 (1979).
[4] J. V. Sanders, Chemica Scripta **14,** 141 (1979).
[5] G. R. Millward, J. Catal. **64,** 381 (1980).
[6] J. M. Thomas, Ultramicroscopy **8,** 13 (1982).
[7] M. J. Yacaman, D. Romeu, S. Fuentes, and J. M. Dominguez, J. Chem. Phys. **78,** 861 (1981).
[8] R. Burch, J. Catal. **71,** 348 (1981).
[9] C. Y. Wang, R. A. Wu, and L. W. Lin, J. Catal (China) **4**(3), 17 (1984).
[10] W. M. Meier, Advan. Chem. Ser. **121,** 39 (1973).
[11] J. M. Thomas, G. R. Millward, S. Ramdas, L. A. Bursill, and M. Audier, Faraday Discussion **72/20,** 3.
[12] C. X. Wang, B. S. Dou, S. R. Fan, Z. L. Yu, Y. F. Xie, and Y. Wu, Science Sinica **B 3,** 209 (1984).
[13] A. Nielsen, Catal. Rev. **23,** 17 (1981).
[14] L. A. Bursill, E. A. Lodge, and J. M. Thomas, Nature London **286,** 111 (1980).
[15] K. Ishizuka, Acta Cryst. **A 38,** 773 (1982).
[16] G. W. Qiao, J. Zhou, and K. H. Kuo, Proc. 8th Intern. Congr. Catal., West Berlin 1984, Vol. 3, p. 93.
[17] G. W. Qiao and B. C. Wang, Proc. 3rd Asia Pacific Conference on Electron Microscopy, Singapore 1984, p. 226.
[18] G. W. Qiao, to be published.